

Adverse Rotorcraft-Pilot Coupling: Test Campaign Development at the University of Liverpool*

M. Jump and S. Hodge[†], B. Dang Vu[‡], P. Masarati, G. Quaranta and M. Mataboni[§], M. D. Pavel^{**}, O. Dieterich^{††}

Abstract

The development of a pilot-in-the-loop investigation into rotorcraft-pilot coupling are presented for three test campaigns which were conducted at the University of Liverpool (UoL) as part of GARTEUR HC(AG-16): rigid body; biodynamic and aeroelastic. For each campaign, the modelling activities and initial results are outlined. PIO events were recorded during the rigid body test campaign, although not always in the expected vehicle axes. The biodynamic campaign required a significant amount of development work to be carried out on the UoL's flight simulation facility and the results of this development are presented. For the aeroelastic campaign, an aeroelastic rotor and slung load were successfully implemented but an aeroelastic fuselage presented problems. The test campaigns are set in the context of being the first step in understanding and preventing rotorcraft-pilot couplings but the paper provides recommendations on the next steps to take the research forwards.

* Submitted to the 34th ERF, Liverpool, Sept 2008

[†] Flight Science and Technology Research Group, The University of Liverpool. Corresponding author **Email:** mjump1@liv.ac.uk, steve.hodge@baesystems.com. **Tel:** +44 151 794 6845; **Fax:** +44 151 794 6841.

[‡] ONERA, Base Aérienne 701, FR-13661 Salon de Provence, France, binh.dangvu@onera.fr.

[§] Politecnico di Milano, Via La Masa 34, I-20156 Milano, Italy, masarati@aero.polimi.it, quaranta@aero.polimi.it, mataboni@aero.polimi.it.

^{**} Delft University of Technology, Kluyverweg 1, NL-2629 HS Delft, The Netherlands, m.d.pavel@tudelft.nl.

^{††} Eurocopter Deutschland GmbH, D-81663 Muenchen, Germany, oliver.dieterich@eurocopter.com.

1. Introduction

Though aviation-related engineering science has progressed immeasurably over the last century, some issues encountered by the Wright brothers in their Flyer still persist today. Descriptions of their early flights suggest that they experienced pitch oscillations that were pilot-induced (Ref. [1]). The reconstruction of the flights of the Wright Brothers' aircraft using piloted simulation at the University of Liverpool (UoL) demonstrated their strong propensity to enter so-called Pilot-Induced Oscillations (PIO, Refs. [2, 3]). PIO are a particular form of what have come to be defined, perhaps more correctly, as Aircraft-Pilot Couplings (APC). Ref. [4] defines APC events as “...*fundamentally interactive and occur during highly demanding tasks when environmental, pilot or aircraft dynamic changes create or trigger mismatches between*

actual and expected aircraft responses”. Ref. [4] further refines this definition by splitting APC phenomena into 3 categories: Category I, which are essentially pilot-aircraft system oscillations; Category II, which are quasi-linear pilot-aircraft system oscillations with rate- or position-limiting present and Category III, which are highly non-linear pilot-aircraft system oscillations. There are many high profile examples of fixed-wing APC events occurring, usually late in the development cycle of a particular vehicle (Space Shuttle Orbiter pitch oscillations on approach to land, SAAB Gripen pitch oscillation on landing, Lockheed-Martin YF-22 pitch oscillation on take-off). The common factor in the examples given so far, from the Wright Flyer to the YF-22 is that they are fixed-wing aircraft. The vast majority of the research effort applied to APC phenomena is for this class of aircraft. Rotary-

wing aircraft, however, are also vulnerable to APC (for this paper, rotorcraft APC will be called rotorcraft-pilot coupling events, or RPC). Indeed, rotorcraft can be particularly vulnerable to RPC events given their limited stability, low values of response bandwidth and the coupling of rigid-body modes with fuselage and rotor aeroelastic modes (Ref. [5]). Of the 203 pages contained in Ref. [4], only 4 are dedicated to rotorcraft. Given the apparent dearth of knowledge with respect to RPC, a multi-disciplinary action group (AG) was set up in 2005 under the leadership of the Group for Aeronautical Research and Technology in Europe (GARTEUR) with the goal of establishing an increased knowledge base to help understand and prevent adverse and dangerous RPC phenomena. The Group had originally divided the work into two major groups. The first, termed 'rigid-body', dealt with an 'active' pilot who was 'keen' to perform a given flying task with motion up to a frequency of approximately 1.0Hz being considered. The second, termed 'aeroelastic', dealt with motion frequencies between approximately 2.0 and 8.0Hz. This activity, as far as the testing at UoL was concerned at least, again involved an active pilot, but this time flying a helicopter model that included rotor and fuselage elastic modes of vibration. A third tranche of activity arose, termed 'biodynamic', and was concerned with a passive simulator occupant, not involved in a flying task. Of specific interest here was the response of the occupant to pre-defined vibratory regimes. This paper is one of four that deals with the results and outcomes of GARTEUR HC(AG-16). Ref. [6] presents an overview of the work carried out including the aims and objectives of GARTEUR HC(AG-16). Refs. [7, 8] present more detailed results for the rigid body and aeroelastic research efforts. Ref. [9] also provides further results analysis from the biodynamic testing undertaken during the action group activities. The common theme throughout the majority of the research activities was for theoretical results to be either validated or tested using pilot-in-the-loop simulations. The Bibby flight simulator at UoL was used for these purposes and this paper presents both the development work that had to be undertaken in order that the

requirements of the GARTEUR test campaigns could be met and a number of the key results that were obtained during the testing process. The paper concludes with a small number of lessons learned and recommendations from the research activity.

2. Rigid Body Test Campaign

2.1 Overview

The primary tool used for the pilot-in-the-loop RPC test campaigns was the UoL Bibby flight simulation facility. This comprises an enclosed pilot station with five outside world and one instrument panel visual channels. This sits on a six degree-of-freedom (dof) motion base. Fig. 1 shows the simulator facility and Refs. [10, 11] provides more details about its geometry, capabilities and usage.



Fig. 1. Bibby flight simulator at UoL

2.2 Aircraft Modelling

The usual *modus operandi* for flight simulation tasks at UoL is based around the creation and use of non-linear multi-(rigid) body dynamics-based air vehicle models using Advanced Rotorcraft Technology's FLIGHTLAB (Ref. [12]) modelling tool. UoL already had such a model of the project helicopter, the BO105, from previous projects (see, for example, Ref. [13]). However, for the rigid-body test campaign, it was decided that a non-linear state-space representation of the model would facilitate analysis by all partners in the project. To try to ensure that pilot-in-the-loop analysis

was consistent with off-line analyses and to allow real-time flight simulation trials to take place, the state-space model had to be created within the FLIGHTLAB environment.

The off-line BO105 models used are described in detail in Ref. [7]. To summarise, two models were used for the trial work ('Baseline' and 'Augmented') at two flight conditions (hover and 65knots). The 'Baseline' model is an identified state space model that includes non-linear terms due to gravity and both inertial and flight dynamics couplings. The 'Augmented' model is the Baseline model with a full authority rate command, attitude hold control system added to it. This provided a helicopter model with the cross-coupling characteristics removed. These models were provided to UoL in MATLAB/Simulink[®] format and this naturally lends itself to model development within FLIGHTLAB's Control System Graphical Editor (CSGE). A dummy FLIGHTLAB model was created that contained the correct vehicle mass and inertia properties. CSGE was used to solve for the model states and calculate the resultant vehicle forces for a given pilot inceptor input. These forces were then applied to the dummy model's centre-of-gravity (cg). The only major point to note was that 'gravity' had to be removed from the initial model calculations since, for any initial condition there is no force calculated to counteract the vehicle weight. The model used was therefore akin to a 'perturbation from initial conditions' model. Fig. 2 shows an example response comparison between the ONERA-supplied and UoL-developed Baseline BO105 models to a longitudinal cyclic input in the primary response axis. Whilst small differences are apparent towards the end of the response, these

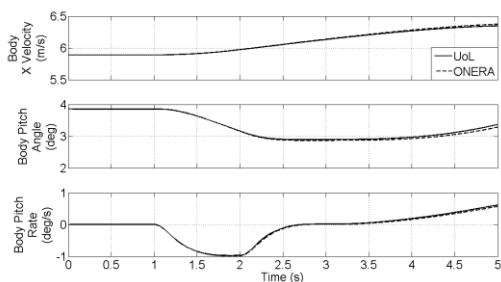


Fig. 2. BO105 model response comparison to a longitudinal cyclic step input

were considered to be sufficiently small to be able to proceed with the planned testing.

2.3 Test Course Design

A number of rigid-body manoeuvres were conducted during the test campaigns. These manoeuvres were selected to ensure that the pilot undertook some control task/activity in each of the vehicle axes with the intention that this activity might drive the pilot-vehicle system into an RPC event. The tasks performed were (in no particular order):

- Vertical manoeuvre (with external gust disturbances present).
- Roll command tracking task (no gust disturbances present).
- Slalom pole course (no gust disturbances present).
- Lateral side-step task (no gust disturbances present).
- Boundary avoidance tracking task (no gust disturbances present).

Two pilots were available for the research project and each pilot flew the courses at least twice. The test courses used for these tasks will be described further in the following Sections.

2.3.1 Vertical Manoeuvre

Ref. [14] defines a 'Vertical Manoeuvre' that simulates a military helicopter unmasking itself and then re-masking itself for tactical reasons. This manoeuvre was implemented in the UoL simulation facility, based upon a version of the hover manoeuvre test course defined in Ref. [14]. Fig. 3 defines the test course used (all dimensions in feet). The pilot's task is to hold

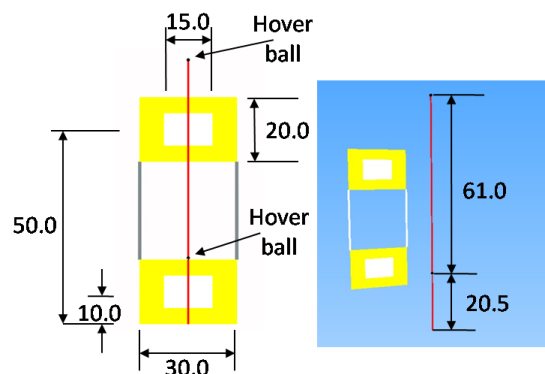


Fig. 3. Hover board task course definition

the hover ball within the confines of either the inner or the outer rectangles defined by the boards.

The aircraft model was started in a trimmed hover-condition at the lower hover board. The pilot was asked to hold this condition for 5 seconds once gust disturbances were added to the simulation and then reposition vertically to a stable hover condition at the upper hover board, again for a period of 5 seconds. Once the pilot declared the condition to be stable, the simulation run was stopped. Fig. 4 shows a representation of the pilot's-eye view of the course when positioned at the lower hover board. The course itself consists of 3D-models generated using Presagis' (formerly Multigen-Paradigm's) Creator software in the standard OpenFlight® format. These are then placed within an outside world database that is stored in OpenGL Performer™ binary format.

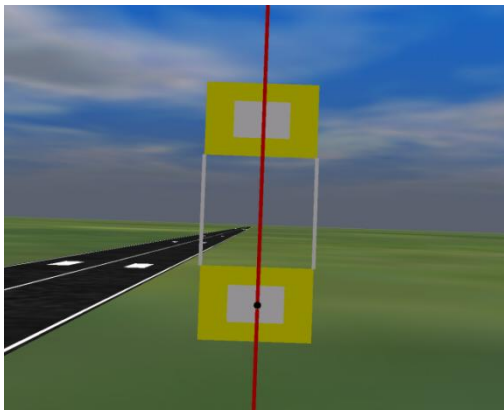


Fig. 4. Pilot's-eye view of the hover course

2.3.2 Roll Command Tracking

The roll command tracking task was inspired by work conducted in Ref. [15]. Fig. 5 shows how the task was implemented at UoL. A simple Head-Up Display (HUD) was developed using Presagis' (formerly Engenuity Technologies) VAPS® software, consisting of the following symbols:

- Aircraft Bar. This bar remains fixed to the aircraft body axis and provides an indication to the pilot of the aircraft roll angle in relation to the outside world.
- Command Bar. This bar is independent of the aircraft body axis

and is fixed with respect to the inertial or earth axis system.

- Adequate Performance Marker Bars. These bars are set at an angle of $\pm 8^\circ$ to the centre of the aircraft bar and would flash from between two and zero seconds prior to the next command bar angle change.

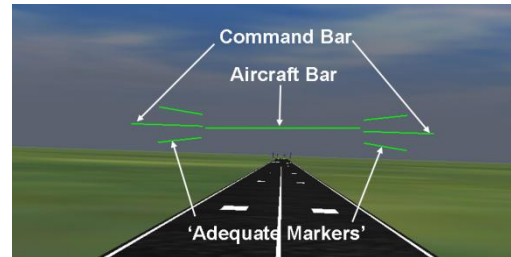


Fig. 5. Roll command tracking symbology

The pilot's task was to maintain alignment between the aircraft and command bars as far as practicable. The 'alignment' was judged to be satisfactory if the aircraft bar lay between the adequate performance marker bars. This level of alignment had to be achieved prior to the adequate bars starting to flash. The command bar sequence was pre-determined and four different sequences were used:

- 'R1' (initial roll to the left);
- 'R2' (roll angles opposite sign to 'R1');
- 'R1L' (as per 'R1' but duration between commanded angle changes doubled) and
- 'R2L' (roll angles opposite sign to 'R1L').

Fig. 6 shows roll command sequence R1.

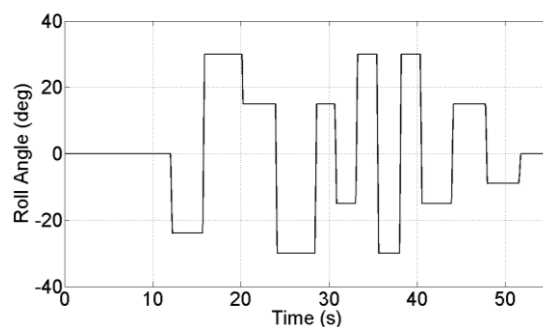


Fig. 6. Roll command sequence R1 for tracking task

2.3.3 Slalom Course

Ref. [14] defines a slalom course layout for the purposes of rotorcraft handling qualities assessment. This was implemented within the UoL simulation facility. To provide an extra level of flexibility for the RPC test campaign, a slalom pole course was developed where the intra-pole distance could be changed by the simulator operator, without the need to change aircraft model, outside world database or in any way curtail the flow or rate of test sorties. Fig. 7 shows a pilot's-eye view of the slalom course. The pilot's task here was to guide the

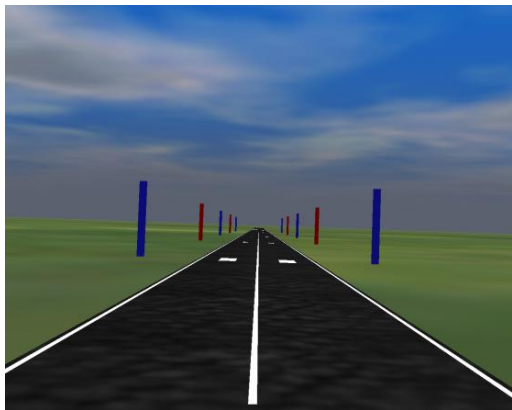


Fig. 7. Slalom course implementation

rotorcraft model between the runway edge and the pole location at the pole's longitudinal runway position whilst maintaining height and speed as per the start condition values.

Based upon initial test-pilot feedback during the work up to the actual trials, for the 'live' test campaigns, three intra-pole distances were eventually used to provide 'low', 'medium' and 'high' workload tasks for the vehicle model in use: 850ft, 700ft, 550ft. As with the hover board course, the poles were individual instances of a 3D model generated in the Creator[®] software.

2.3.4 Lateral Side-Step

Ref. [14] defines a side-step course layout for the purposes of handling qualities assessment. A version of this course was implemented in the UoL simulation facility and is defined in Fig. 8 and Fig. 9 (all dimensions in metres). The pilot's task was to fly from a stable hover to a stable hover laterally, maintaining separation distance from the crane gantries and

height. The manoeuvre start and finish positions were overhead the square boxes with the top bar of the crane aligned with the (red) cross on the gantry behind it (Fig. 9). It required acceleration into lateral flight to initiate the manoeuvre and then an opposing deceleration manoeuvre back into the hover. The lateral manoeuvre tasks were carried out to both the left and the right.

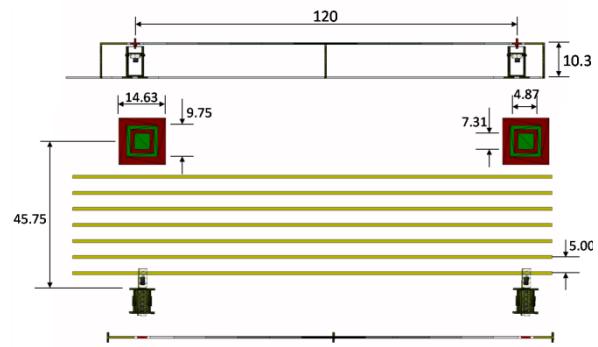


Fig. 8. Lateral side-step course definition

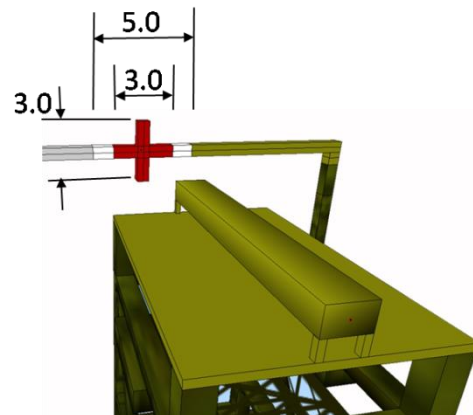


Fig. 9. Lateral side-step alignment detail

2.3.5 Boundary Avoidance

The boundary avoidance tracking tasks required the pilot to use the aircraft boresight on a VAPS-developed HUD to follow an oscillating pitch command symbol. Two pitch angle boundary symbols (upper and lower) were also included on the HUD.

Fig. 10 shows the implementation of the boundary tracking experiment HUD generated using VAPS[®].

Two variations of this experiment were conducted:

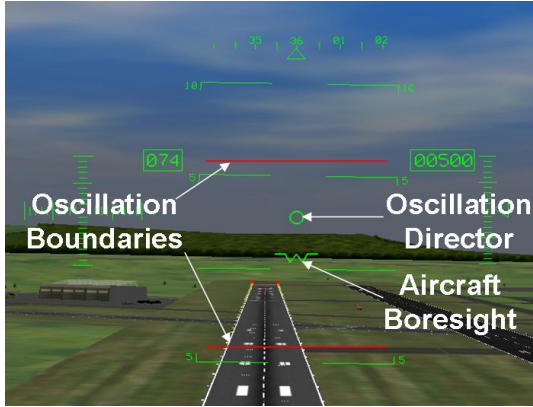


Fig. 10. Boundary avoidance task HUD symbology

- The director symbol oscillated sinusoidally between the two boundary limits. The boundaries were initially fixed but for a second round of testing became increasingly ‘narrow’ at a pre-determined rate (see boundary pitch angle limits below).
- The director symbol oscillated following a pre-determined sum-of-sines path, within the limits of the boundary markers which, again, became increasingly narrow at a pre-determined rate. This experiment was performed to try to prevent the pilot being able to ‘predict’ the motion of the oscillation director. In order to increase the ‘danger’ of the boundaries, an automatic count of boundary exceedances by the pilot was made. Once this number exceeded an agreed limit (5), a stall-warning sound was played into the simulator pod. This ‘nuisance’ sound was intended to ensure that the pilot did indeed try to avoid the boundaries presented to him.

The boundary pitch angle limits used were: $\pm 14^\circ$; $\pm 8^\circ$; $\pm 5^\circ$; $\pm 3^\circ$ and no boundary (‘sum-of-sines’ experimental variation only). For the sinusoidal test cases, the frequency of flight director oscillation was also varied at 0.25, 0.375 and 0.5Hz.

Fig. 11 shows the basic command profiles used to drive the oscillation director. For the sinusoidal test cases, the amplitude was then multiplied by the boundary pitch angle limits. For the ‘sum-of-sines’ experiment, the

oscillation amplitude was multiplied by an empirically determined factor of 4.0. This multiplying factor gave a balance between a typical helicopter pitching motion and a close approach to the encroaching oscillation boundaries.

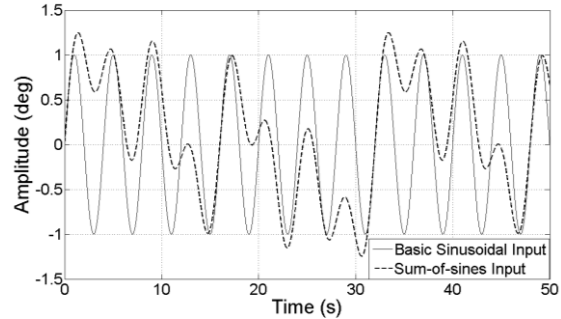


Fig. 11. Oscillation director command signals

2.4 Test Results

The following Section highlights a number of the more interesting test results obtained during the GARTEUR HC(AG-16) rigid-body test campaigns. Each manoeuvre was flown by the pilot and then given a subjective assessment using the PIO rating scale of Ref. [16]. A version of this rating scale is shown in Appendix A.

The results presented herein are the ‘raw’ data recorded directly from the simulation. The primary analysis and elaboration of these data is presented in Ref. [7].

2.4.1 Vertical Manoeuvre

Fig. 12 shows an example vertical manoeuvre response in the Augmented aircraft where pilot 2 rated the manoeuvre with PIO Rating (PIOR) 4 in the heave axis. Fig. 13 shows the yaw

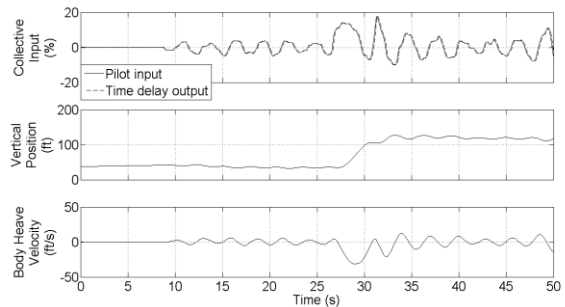


Fig. 12. Augmented model heave response to vertical manoeuvre with 100ms time delay introduced into collective control circuit

response for the same manoeuvre where the pilot reported PIOR 6 for the yaw axis.

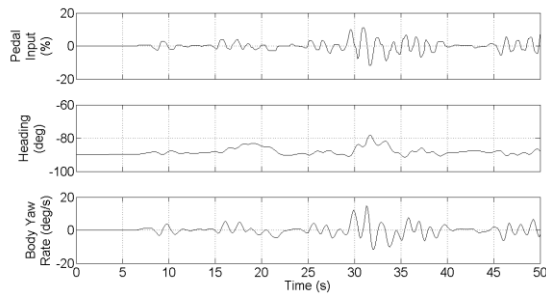


Fig. 13. Augmented model yaw response to vertical manoeuvre with 100ms time delay introduced into collective control circuit

The pilot reported that he was unable to maintain position satisfactorily and that the high vertical speeds capable with this model meant that he had to be very aggressive on the collective. The yaw axis PIO was unexpected in the sense that the augmented model was ‘decoupled’. It was initially suspected that the yaw control path had saturated but this was not the case in this example (it had been in others). The likely explanation is that the model is not entirely decoupled, particularly for aggressive control inputs. When the pilot is very much in the loop trying to obtain and maintain position at the top of the hover course (at around 28-35s), it appears that an attempt to maintain heading has triggered a number of more significant oscillations in the yaw axis.

2.4.2 Roll Command Tracking

Fig. 14 shows an example of the most severely rated roll tracking test sortie, rated by pilot 1 at PIOR 5, in the roll axis. Both pilots reported having to continuously ‘hunt’ for the correct roll angle and that they were never really able to ‘settle down’. This is perhaps most apparent in the lateral cyclic trace of Fig. 14. There is less evidence of task abandonment or even divergent oscillations in the results which would result in a PIOR of 5. However, the pilot may have felt that he was abandoning the task since for many of the roll commands, he only just/never manages to achieve the roll angle before being commanded onto the next one. At this point the symbology would be flashing to indicate that the task should already have been achieved. There are a number of

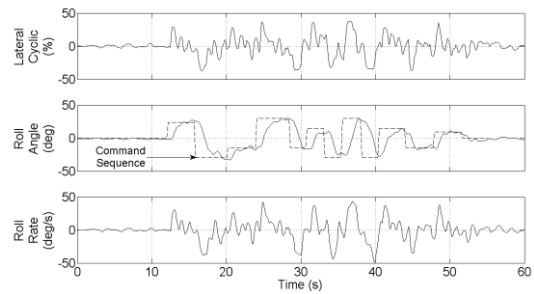


Fig. 14. Baseline aircraft model roll tracking test point, PIOR=5, roll task R1, no time delay or rate limits present

cases where the commanded roll angle is not reached before the next angle has to be selected. In this sense, the task of obtaining the previous roll angle has been abandoned.

2.4.3 Slalom

Fig. 15 shows an example of a PIOR 6 (yaw axis) slalom test point flown by pilot 2. This rating was provided for the Baseline aircraft model with no time delays present in any of the pilot command pathways.

Of all of the manoeuvres chosen, the slalom

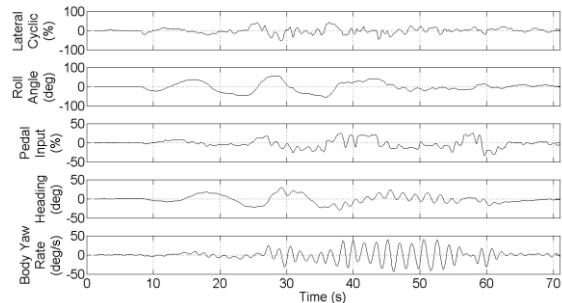


Fig. 15. Baseline aircraft model slalom with PIOR 6, pole separation distance 700ft, no time delays present

task is the least targeted at a particular flight axis as control actions are required in all of them. However, it was still somewhat of a surprise that the worst case PIO was reported in the yaw axis. The oscillations start just over half-way through the slalom course but the worst of them was triggered as the pilot attempted to re-align the flight path with the runway centre-line. Only after some 20 seconds is yaw axis control re-established.

2.4.4 Lateral Side-Step

Fig. 16 shows a lateral side-step manoeuvre that was awarded PIOR 5 in the roll axis by pilot 1. This manoeuvre was carried out using the Augmented BO105 model with a 37.5%/s rate limit introduced into the control command path. The aircraft has a small oscillation throughout the manoeuvre but the major PIO event is triggered as the pilot tries to halt the lateral translation at the far end of the course.

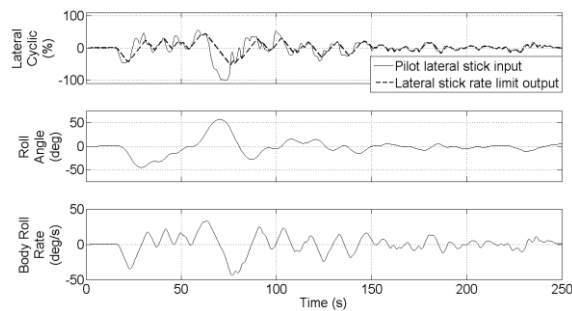


Fig. 16. Augmented aircraft side-step manoeuvre with PIOR 5 in the roll axis

The effect of the rate limiting in the command path can clearly be seen in the lateral cyclic trace of Fig. 16. The aircraft roll rate also shows the typical ‘saw-tooth’ characteristic of a rate-limited Category II PIO.

2.4.5 Boundary Avoidance

Fig. 17 shows an example of the results from the sinusoidal-type of excitation from the boundary avoidance tracking test campaign. This run was awarded a PIOR of 5 by pilot 2 in the pitch axis. The flight director amplitude was $\pm 5^\circ$ and the frequency of oscillation 0.5Hz.

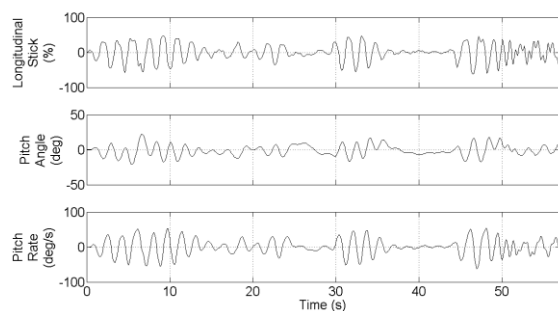


Fig. 17. Baseline aircraft boundary avoidance tracking test sortie with PIOR 5 in pitch axis

The pulses of oscillations within the response traces are the result of the pilot attempting to engage with the task of following the oscillation director. The resultant aircraft oscillation quickly increases in amplitude and after a number of cycles, the pilot abandons the task to make another attempt. This task was a very good example of how to drive the pilot-vehicle system into a limit-cycle/unstable response situation with a seemingly innocuous manoeuvre.

3. Biodynamic Test Campaign

3.1 Overview

The rigid-body test campaign had forced a departure from the usual ‘normal operations’ of the Bibby flight simulation facility in terms of a ‘new’ method of vehicle modelling being used for real-time simulations and the development of a number of new (to UoL) test courses and HUDs. The requirements of the biodynamic (and aeroelastic) test campaign(s) forced a much more radical set of developments to be implemented in order that the planned testing could be conducted.

Ref. [9] describes the test campaign in more detail. In summary, the objectives of the biodynamic testing were twofold: 1) to obtain transfer functions for pilot limb responses at various control inceptors (primarily the collective lever) and compare with the available literature (see, for example, Ref. [17]) and 2) begin to develop a multi-body dynamics pilot model for use in future RPC studies. This was to be achieved by exciting ‘pilots’ in the Bibby simulator and measuring the response of their limbs to this vibration.

To achieve these objectives, the biodynamic test campaign called for the following developments:

- The ability to apply motion demands directly to the motion base;
- Measurement of the actual excitation experienced by the pod occupant;
- Measurement of the resultant limb and control inceptor responses to the applied excitation.

- A means to record all of the data being recorded from the various sources.

The following Section provides more detail on each of these items.

3.2 Test Campaign Requirements Delivery

FLIGHTLAB is delivered with a utility that enables data blocks to be written from and read in to models and enables the broadcasting of these data across a network ('flcomms'). This utility was used extensively during the preparation for the biodynamic and aeroelastic test campaigns. In the following Sections, when a data item is referred to as being broadcast, this was achieved using 'flcomms'. Unless otherwise stated, the recording rate for the data was 0.01s or 100Hz.

3.2.1 Simulator Base Motion Demand System

Until the requirements for the test campaigns of HC(AG-16) arose, the motion system in the Bibby simulation facility had been used as a 'black box' by UoL. That is to say, most of the research concentrated on development of high fidelity multi-body flight dynamics models and the driving of the motion base when these were used was left to the 'turn-key' solution provided as part of the installation.

The motion base is driven by proprietary software (MB-MOVE) provided by Motionbase (now part of QinetiQ). A new version of this software was compiled that had the following additions made to it:

- Read in the current state of the 'model' being used to drive the motion base e.g. 'Run', 'Pause', 'Reset' etc. These states were used not only to stop/start the excitation demand being applied to the simulator motion base but also to trigger the data recording and file writing process.
- Broadcast the platform motion and actuator servo demands. These were used to validate a model of the motion base described later in this Section.

The motion base driver software requires 6 data items as input. These are termed the 'Specific Forces' which are: 1) three linear acceleration components (surge (fore-aft), sway (left-right) and heave (up-down)) and 2) three rotational rates (pitch, roll and yaw). In order to provide these to the motion base driver software, which was 'listening' on the network for a specific data block ('MOTIONBASE') containing these data, a dummy FLIGHTLAB model was created. In simple terms, this model read in the required excitation demand from a text file and then wrote it out again to the MOTIONBASE data block which was then broadcast across the simulation facility network. Fig. 18 shows an example excitation demand in the heave axis. It is the first part of a 0.2g sinusoidal frequency 'sweep' from 0.4 to 7.0Hz. The sweep is not smooth but is stepped in increments of 0.2Hz after 25 cycles at each frequency. In this instance, all other axis demands were set to zero. The other kind of excitation that was applied was a randomised vibratory demand. Two (nominal) peak amplitude levels were investigated, ± 0.1 and $\pm 0.2g$.

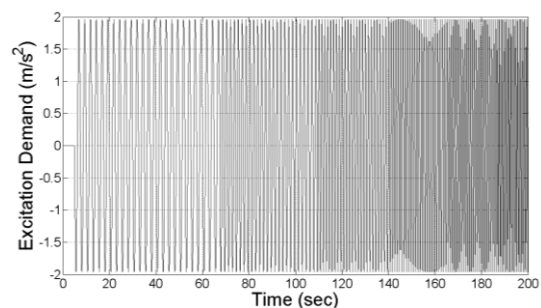


Fig. 18. Example biodynamic heave excitation demand

Given that this was the first time that the Bibby simulator had been used in this manner, it was desirable to be able to verify, in some way, that the demands to be made on the motion base were not going to be beyond its capabilities. To that end, a model of the motion base cueing algorithms was constructed and the planned excitations passed through it. The predicted response was then compared with the published capabilities of the motion platform. Fig. 19 shows the predicted heave response of the platform to the excitation of Fig. 18. This response is typical in that, as for all of the planned cases, the model showed that the vibration demand was well within the limits of

the motion platform. It also shows that the desired excitation amplitude is predicted to never actually be achieved and that the actual excitation levels at the lowest frequencies will be significantly less than that demanded. This was both expected (given the transfer functions of the motion base filters) and not considered to be a particular issue. Provided that the actual excitation amplitude was known by measurement, the experimental objectives could still be achieved.

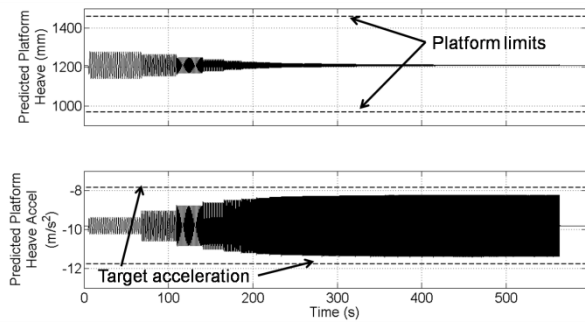


Fig. 19. Motion base model predictions to 0.2g heave excitation: (a) platform heave response and (b) platform heave acceleration

Whilst the motion base modelling provided the required confidence to proceed with the testing, there was still some need for caution. The motion platform driver software was modelled using all of the available published information (Ref. [18]). However, the motion system also contains a Motionbase proprietary safety system that is intended to protect the base from inadvertent damage. No information is available for this ‘adaptive filtering’ and hence could not be included in the motion base model. Whilst its exclusion from the modelling process should only have led to the conservative predictions, the actual testing was approached such that any risk to hardware or personnel was minimised as follows:

- All excitations were applied to the pod with no occupant prior to the test campaigns.
- Excitations in any given axis/combinations of axis were always applied with the lowest amplitude first.

During the initial phase of excitations with no occupant, a small number of what appeared to be pod-motion base resonances were detected at the upper range of excitation frequencies in

the surge and sway directions. The GARTEUR test campaign concentrated primarily on the heave axis but for the cases where these phenomena were detected in other axes, the excitation definitions were curtailed prior to this frequency being reached.

3.2.2 Simulator Base Motion Measurement

In order to measure the actual excitation being experienced by the pod occupant, a MicroStrain® 3DM-GX1® motion sensor was procured by UoL. The sensor was mounted as shown in Fig. 20 on the simulator motion base frame. Fig. 20(a) indicates the sensor location which is behind, below and set back from the pilot seat in the pod. The sensor unit was bolted to a 5mm steel plate which was then

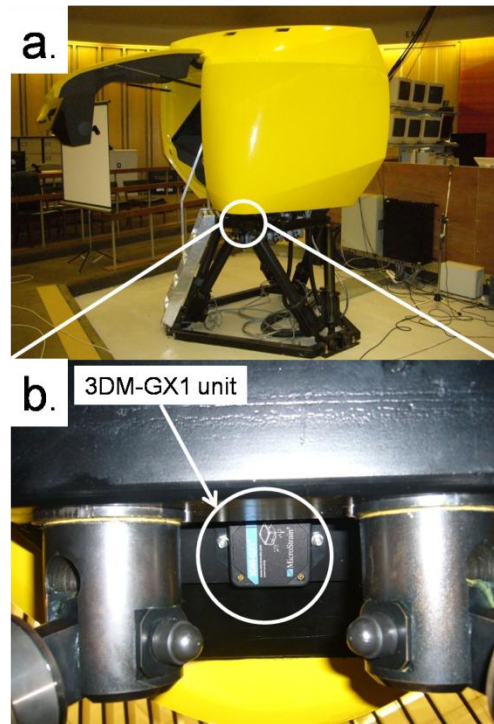


Fig. 20. MicroStrain 3DM-GX1® motion sensor mounting location

fastened to the motion base using existing bolts that secure the simulator pod to the motion base frame. Fig. 20(b) shows the 3DM-GX1® unit mounted in place. It shows the view ‘looking up’ from the floor below the mounting plate. This was considered to be the most ‘rigid’ location that was the also the most accessible for mounting purposes. Strictly speaking, the measured excitation is not necessarily that being experienced by the occupant directly. The excitations applied

during the test campaign were nominally purely linear and so the fact that the motion sensor was not mounted at the centre of rotation of the motion base is not an issue. However, the occupant sits on a foam seat (the foam is approximately 10mm deep) and the seat is securely bolted to the metal base frame but sits on top of a wooden floor panel inside the simulator pod. It was considered however, given the resource and time limitations of any GARTEUR activity that the solution used would be acceptable for the testing to be performed.

In order that the 3DM-GX1[®] could be of use to the test campaign, a specific program was written (in C) to request that the device output measured linear acceleration, rotational rate and angular measurement data (1 per axis so 9 data values in total). These data were then broadcast in a data block across the facility network ('ACCELEROMETER').

3.2.3 Pod Occupant Limb and Control Position Measurement

The requirements for the testing specified that both control inceptor and occupant arm positions be recorded for any given excitation. Because the excitation was being passed through a FLIGHTLAB model (albeit a 'dummy' one), then stick positions were automatically generated during a real-time run. These data were simply added to a data block and broadcast across the simulator network ('STICKPOS'). Much of the testing conducted was concerned with the collective lever and specifically the collective lever with its friction set to its minimum value. With this setting in place, the collective became 'floppy', yet the test plan called for the pilot to maintain the stick position at 10%, 50% or 90% of its full scale deflection (fsd) for a given test point. This presented a further problem in that the stick trim positions are all 'relative' to their position when the simulation is started. Thus, if the collective trimmed position was (say) 46% and a simulation run is started with the lever at its lowest position, then the pilot would not be able to achieve any value lower than 46%, only values greater than this. The planned testing called for the position of the controls to be known in absolute, rather than relative terms.

To solve this latter problem, a series of wooden 'jigs' were constructed for the required 10%, 50% and 90% start positions such that the start position of the collective was the same for each test point. In order that this position could be maintained during an excitation test run, a VAPS[®] HUD was constructed, as shown in Fig. 21, which was displayed to the pod occupant. The left-most symbol (XC) displays collective position, the centre cross-shaped symbol (XA, XB) shows lateral and longitudinal cyclic position respectively and the right-most symbol (XP) provides pedal position information. The occupant was instructed to passively hold the control inceptors (no flying task was conducted) and only to intervene if the control position deviated from the nominal start position by greater than $\pm 10\%$.

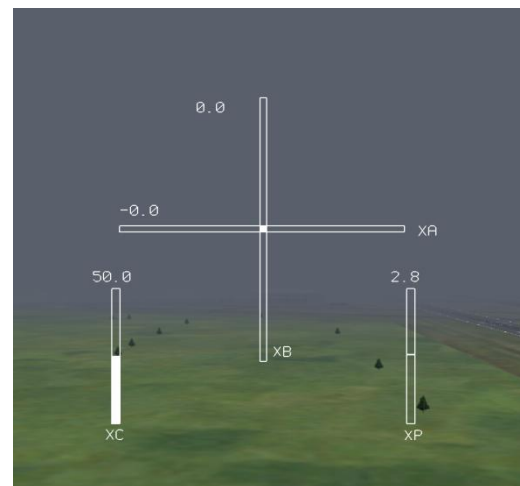


Fig. 21. Control inceptor position HUD

Limb positions (wrist and above the elbow) were measured using two Xsens MTx motion sensors procured by Politecnico di Milano (POLIMI). Fig. 22 shows a typical set-up for these devices prior to the commencement of a test run. The two MTx sensors were secured to the occupant using elastic fasteners, similar to those in use with the medical profession. Also visible in the figure are the previously mentioned wooden jigs. Once again, a bespoke C program was written (by POLIMI) to interrogate these devices for motion data, to write these data to data blocks and to broadcast these blocks across the simulator network ('MTX1', 'MTX2').

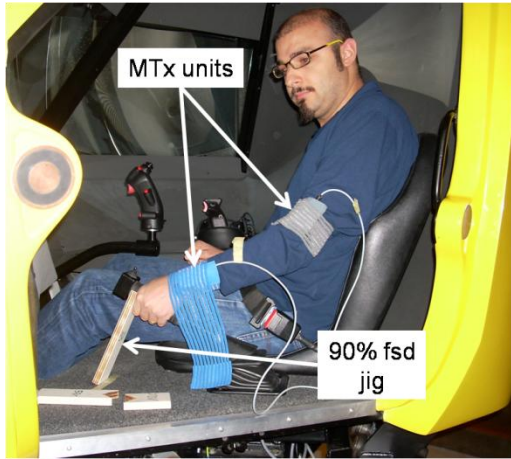


Fig. 22. Illustration of occupant instrumentation for biodynamic testing

3.2.4 Data Recording Solution

In order that the results data of interest was both stored in one place and synchronous, a single computer was used to read in the various data blocks being broadcast across the simulator network. A C program was created for this task. When a simulation run was started or 'Run', the recording program would start to read the data into a buffer. Once the run was commenced and the simulation 'Paused', writing to the buffer was stopped. Only once the simulation was 'Reset' would the data in the buffer be written out to a MATLAB-compatible file format. In order to effect this, a data block SIMSTATE was created to store the simulator run state. For each run, 7 data blocks were recorded. These are MTX1; MTX2; ACCELEROMETER; STICKPOS; KINEMATICSIN; KINEMATICSOUT and MOTIONBASE. Appendix B provides the definitions of and more details about each of the data items in these blocks. Fig. 23 presents comparative plots between the heave displacement command (KINEMATICSIN) and subsequent heave acceleration for the motion base model and for the measured data. It can be seen that the model of the motion base under-predicts the resultant measured acceleration. This was somewhat unexpected as it was believed that the absence of adaptive gain modelling would make the model conservative in this regard. This result however, justified the staged approach to the actual testing that was adopted.

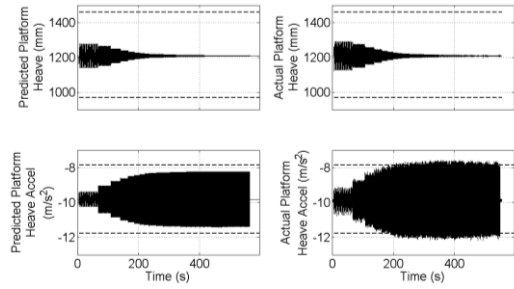


Fig. 23. Comparison of motion base model and measured data

3.3 Sample Results

The system described in Section 3.2 is shown schematically in Fig. 24.

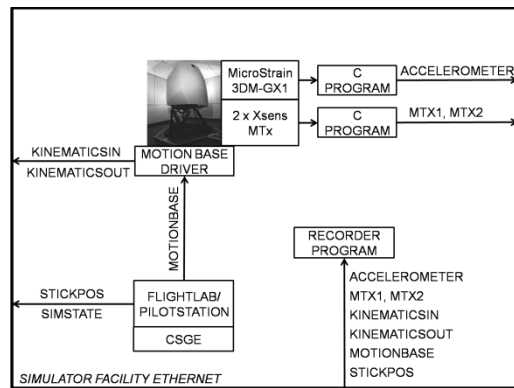


Fig. 24. Schematic of biodynamic test campaign set-up

Fig. 25 shows example data recorded during a $\pm 0.2g$ heave excitation with the collective at 50% fsd test case. It can be seen that, as instructed, the pod occupant resets the collective to the nominal 50% position at approximately $t=320s$ and that a number of small resonances are measured in the occupants limbs as the frequency of excitation is increases e.g. $t\sim 350s$. It should be noted that the recorded collective position is relative to the pod whilst the MTx data is a measurement of absolute limb motion.

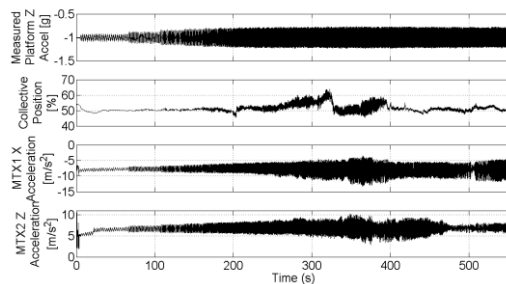


Fig. 25. Sample recorded data from the biodynamic test campaign

More detailed analysis of the results from this test campaign can be found in Refs. [8, 9].

4. Aeroelastic Test Campaign

4.1 Overview

The biodynamic test campaign called for a passive pod occupant to be excited by vibrating the simulator motion base where no flying task was being performed. The aeroelastic test campaign went beyond these requirements in a number of ways:

- The pod occupant would now have to pilot a helicopter model through a low workload task whilst being subject to an increasing feedback from the motion system.
- The helicopter model to be used would have to incorporate aeroelastic rotor and fuselage modes of vibration.
- Time and resources permitting, a slung load should be incorporated into the test program (slung loads have been linked to a number of RPC incidents).

The following Section provides more detail on each of these items.

4.2 Test Campaign Requirements Delivery

4.2.1 Aeroelastic Piloting Task

The planned aeroelastic campaign was intended as an initial assessment to establish whether a simulator facility such as the one at UoL would prove suitable for the assessment of aeroelastic RPC phenomena. With this in mind, it was not considered an efficient use of resources to employ professional test pilots at this embryonic stage of the test campaign. As such, any piloting activity was to be carried out by pilot-engineers which necessitated that any task to be performed was ‘simple’ and low workload. However, the task would have to be sufficiently engaging so that the pilot would not be instantaneously conscious of any inadvertent stick motions being induced by any of the airframe/rotor elastic modes. A simple tracking task was designed whereby the pilot was instructed to follow a sphere that would be oscillating sinusoidally in both/either/none of the heave and lateral directions. The amplitude of the oscillations could be controlled ‘on the

fly’ such that the task could be quickly modified to suit an individual pilot’s skill level. Fig. 26 shows the pilot’s-eye view of this task.

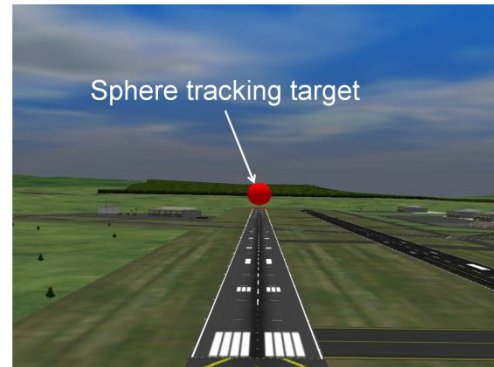


Fig. 26. Aeroelastic simple tracking task

The requirement to provide increasing gains to the motion system was easily met via the use of CSGE. Rate limiter blocks were used to generate a ramp function which could then be used to multiply the demanded specific force being broadcast to the motion base driver software. Fig. 27 shows the effect of this ramping gain in the heave axis demand signal. This test point was flown by an engineer pilot who provided a manual oscillatory collective input to the model.

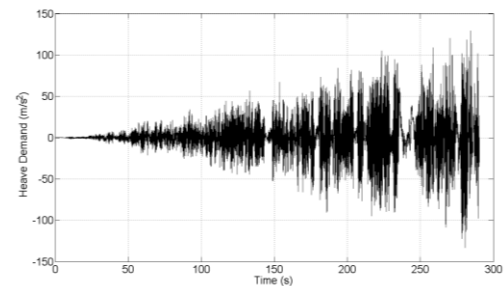


Fig. 27. Effect of increasing gain in the motion feedback loop

4.2.2 Aeroelastic BO105 Rotor Model

The FLIGHTLAB template allows the user to specify the level of detail to be used for the rotors on a rotorcraft model. The user can choose whether the rotor is modelled using blade elements, finite element model data or as a more general rotor disk. The user can then further choose what kind of blade structure for the rotor is to be modelled (articulated, hingeless etc.). Finally, the user can select whether to use a rigid or an elastic rotor blade

model. UoL FLIGHTLAB models tend to be exclusively rigid and so the requirement to develop an elastic rotor model was the next challenge to be tackled. BO105 structural rotor data were provided as described in Ref. [6] by Eurocopter Deutschland GmbH (ECD). Once converted to the appropriate units system, FLIGHTLAB contains a utility that performs a modal reduction analysis and outputs a blade modal data file that is suitable for inclusion in a FLIGHTLAB multi-body dynamics model. Fig. 28 shows a fan plot comparison for the first three rotor modes between the ECD CAMRAD II and UoL FLIGHTLAB models. In order of increasing frequency, mode 1 is 1st lag, mode 2 is 1st bending and mode 3 is 2nd bending.

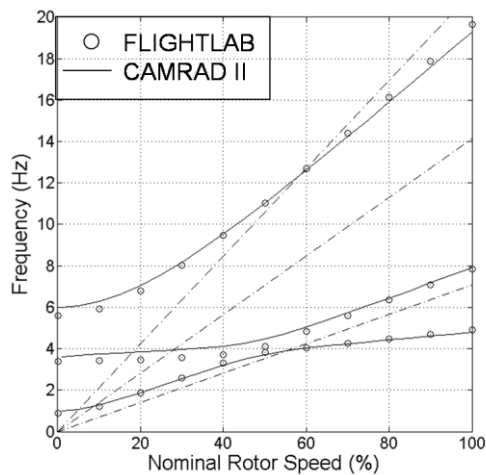


Fig. 28. Fan plot comparison for ECD and UoL elastic blade models

Fig. 29 shows a comparison of the blade shapes in the primary axis for the first three elastic modes of each of these models.

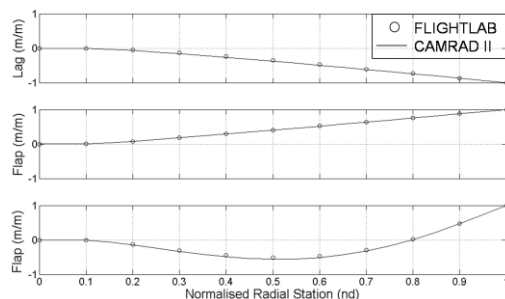


Fig. 29. Elastic blade mode shape comparison between ECD and UoL elastic blade models

The blade mode shapes show excellent agreement. There are some small differences between the blade mode frequencies in the fan plot but there is generally an acceptable level of agreement at the 100% rotor frequency, where the helicopter model was to be used. The differences are perhaps attributable to the differing methods of computation used by the two software packages.

4.2.3 Aeroelastic BO105 Fuselage Model

The FLIGHTLAB model template for a fuselage allows the user to specify whether it be rigid or elastic. All UoL FLIGHTLAB models to date had been rigid and so the requirement to develop an elastic fuselage model meant a departure from FST's traditional areas of expertise. This was compounded by the fact that there are no publically available FLIGHTLAB models containing elastic fuselage models from which to work. BO105 elastic fuselage data were provided, as described in Ref. [6], by ECD. These data were converted into the FLIGHTLAB required tabular format and were then successfully incorporated into the UoL rigid body BO105 FLIGHTLAB model. 'Successful' in this instance means that the data were loaded into the FLIGHTLAB model analysis environment without any errors being detected. This is a pre-requisite if any offline or real-time pilot-in-the-loop analyses are to be conducted. To try to verify that the elastic fuselage model had been implemented correctly, both on- and off-line excitation was applied to the FLIGHTLAB model by means of the pilot control inceptors. The response of the fuselage model was recorded and spectral analyses performed to check the frequency content of the signal. Fig. 30 shows the motion of the fuselage node that represents the pilot's seat in response to an off-line collective sinusoidal sweep between 0.1 and 50.0Hz with rotor modes included (Fig. 30(a)) and excluded (Fig. 30(b)) from the model.

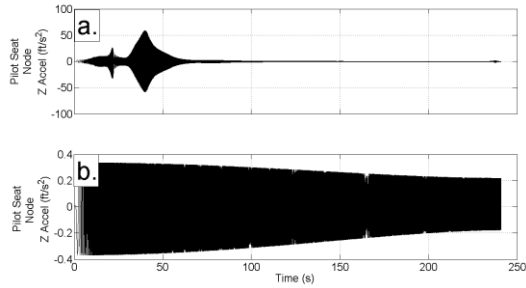


Fig. 30. Pilot seat fuselage node response to collective excitation

Although these responses look promising (the modelled structure appears to be vibrating with some resonances occurring), spectral analysis of the signals did not provide any evidence that the fuselage modal frequencies were present in the model. Following a significant amount of unsuccessful troubleshooting of this problem, it was decided by the relevant project partners, with some disappointment, to postpone this element of the modelling for this phase of testing.

4.2.4 BO105 with Slung Load Model

Due to the issues experienced with the development of the elastic fuselage model, it was decided to implement a slung load model using the UoL rigid BO105 FLIGHTLAB model. It is possible within the FLIGHTLAB model definition to include a number of types of 'External Bodies'. These include external stores, ships and ground planes. Of particular relevance in this case is the ability to add in, with relative ease, a slung load model. Different modelling options are available and the option selected for this preliminary study was a 3-dof slung load with a single segment elastic cable. No aerodynamic loads were included for the brief testing conducted. The load mass was varied to gain some experience in using the sling load model with the cable stiffness set at a fixed value.

4.3 Sample Results

The slung load model testing was the only phase of the aeroelastic pilot-in-the-loop campaign to produce any 'reliable' results and even these are limited in their scope. Fig. 31 shows a hover case flown by pilot 2 with gust excitation present using the rigid FLIGHTLAB BO105 model with a 150kg slung load. The

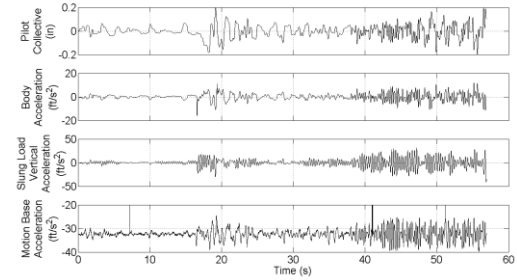


Fig. 31. Hover test case with slung load

pilot was tasked with maintaining a hover at the test run start location for as long as possible. It can be seen that the sling load is contained successfully for some 40 seconds, despite some disturbance that had to be controlled half way through that period. However, stick and load activity do start to build up with divergent pilot input amplitudes observed towards the end of the run. The pilot's comments were that the presence of the sling load could definitely be felt and that he considered himself to be on a 'knife edge' towards the end of the run. The sling load was generating unintended collective motion and was also requiring increasing attention from the pilot to maintain station.

5. Discussion

The UoL Bibby flight simulator has been used during the GARTEUR test campaign for a diverse range of testing purposes. Not all of them have been as successful as had been hoped, but even for those that were, a number of interesting discussion items have arisen. This Section briefly covers each of these topics.

The aeroelastic test campaign was arguably the least successful in achieving its pilot-in-the-loop objectives but was the most high-risk from the outset. None of the partner organisations had extensive FLIGHTLAB aeroelastic modelling experience and in particular, there are no publically available aeroelastic fuselage models to use as a reference when difficulties were encountered (a typical method for generating a model in FLIGHTLAB is to start with a known working model and to modify it with the new model's datasets). However, in attempting this test campaign, a number of positive outcomes were achieved:

- The ease with which sling load models can be generated within FLIGHTLAB and their ability to induce involuntary pilot control inputs was established.
- The means by which to obtain a more successful aeroelastic fuselage model was ascertained.

As such, if this work is to be taken forward, and it is hoped that it will be, this campaign can be considered to be a reasonable risk reduction exercise for the next stage of the work.

The biodynamic campaign was the trigger for the most radical set of developments in the UoL flight simulation facility, possibly since its inception. In preparing for this campaign, the ‘inner workings’ of the facility hardware and software have had to be understood and this has led to a more flexible and agile facility for the future.

The biodynamic test campaign concentrated on the heave axis/collective control but there is still much left to be achieved. The start point for this would be a continuation of this work but looking at excitations in the remaining axes.

The rigid body test campaign successfully generated PIO events in a simulation environment. It required the least facility development but still provided a number of lessons learned. The first was the means by which a state-space vehicle model could be implemented within the ‘standard’ CSGE environment. The second was that however carefully a task is ‘tuned’ to provide an effect in a particular axis, PIO events can potentially occur in any of them.

The rigid-body testing conducted as part of GARTEUR HC(AG-16) is certainly not the

end of the story. Only two pilots were used and two helicopter models. For handling quality ratings work, a minimum of 3 pilots is considered acceptable with 5 being desirable (and if more are available, then so much the better). To increase the validity of any results, the testing should be repeated using more pilots. The use of two helicopter models has provided a useful start point for analysis. However, in order to be able to apply the analysis over a wider range of the existing RPC criteria, further helicopter models with differing dynamic behaviour will be required.

6. Conclusions

This paper has documented the development of and results from the GARTEUR HC(AG-16) investigation into rotorcraft pilot couplings. The main conclusions are summarised as follows.

First, the UoL flight simulation facility was used to successfully trigger PIO events using a non-linear state-space representation of the BO105 using FLIGHTLAB as the real-time simulation tool and professional pilots as ‘men-in-the-loop’.

Second, the simulator facility was successfully adapted to become a ‘shaker table’ in which volunteer subjects were vibrated under varying accelerations to establish their collective arm motion response to such excitation.

Finally, some limited progress was made in the area of aeroelastic modelling in that both an elastic rotor and slung load were successfully modelled in the FLIGHTLAB environment.

The testing conducted is set in the context of it being a first step to understanding the causes and preventative methods for rotorcraft pilot-couplings but further work is required to progress this topic.

Appendix A – Rigid Body Testing PIO Rating Scale

Fig. A1 shows a representation of the PIO rating scale used for the rigid body test campaign.

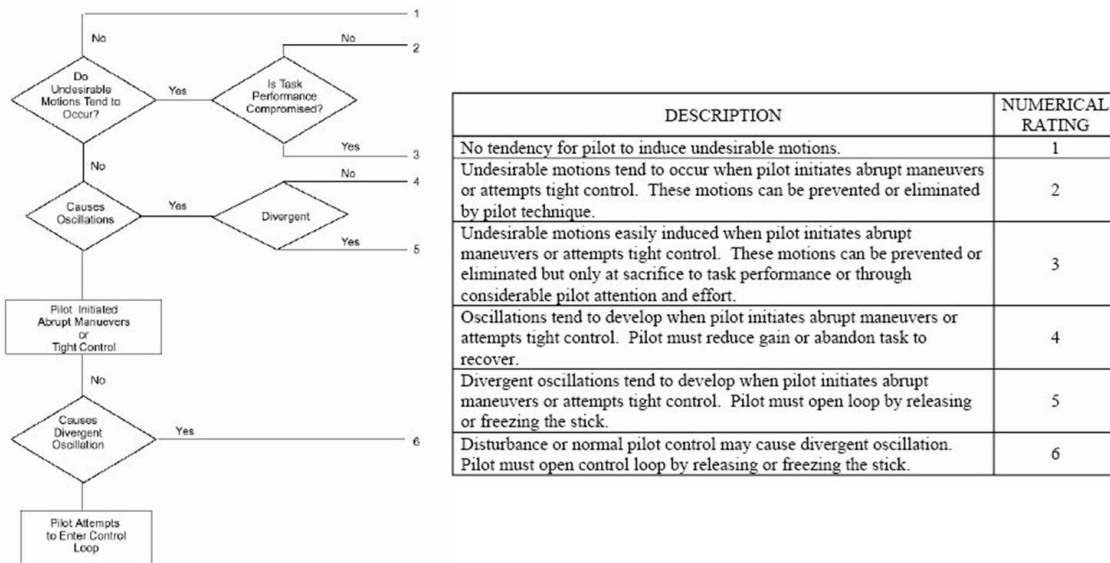


Fig. A1. PIO Rating Scale

Appendix B – Biodynamic Testing

Data Block Definitions

This Appendix provides details of the data recorded for the biodynamic test campaign. The data block name is given in capitals e.g. MTX1 followed by a brief description. The individual data streams within that block is then listed.

MTX1 and MTX2: Pod occupant wrist and elbow motion.

1. Sample count (nd)
2. Temperature (degC)
3. X acceleration (m/s^2)
4. Y acceleration (m/s^2)
5. Z acceleration (m/s^2)
6. X angular rate (deg/s)
7. Y angular rate (deg/s)
8. Z angular rate (deg/s)
9. X Magnetic field (mGauss)
10. Y Magnetic field (mGauss)
11. Z Magnetic field (mGauss)
12. Roll angle (deg)
13. Pitch angle (deg)
14. Yaw angle (deg)

KINEMATICSIN: Motion platform position demand.

1. Platform X position demand (mm)
2. Platform Y position demand (mm)
3. Platform Z position demand (mm)
4. Platform Roll Demand (deg)
5. Platform Pitch Demand (deg)
6. Platform Yaw Demand (deg)

KINEMATICSOUT: Motion platform leg actuator servo demands.

1. Leg 1 actuator servo demand (mm)
2. Leg 2 actuator servo demand (mm)
3. Leg 3 actuator servo demand (mm)
4. Leg 4 actuator servo demand (mm)
5. Leg 5 actuator servo demand (mm)
6. Leg 6 actuator servo demand (mm)

MOTIONBASE: Dummy model motion demand to platform.

1. Specific X force supplied to motion base driver software (m/s^2).
2. Specific Y force supplied to motion base driver software (m/s^2).
3. Specific X force supplied to motion base driver software (m/s^2).
4. Angular roll rate supplied to motion base driver software (rad/s).
5. Angular pitch rate supplied to motion base driver software (rad/s).

6. Angular yaw rate supplied to motion base driver software (rad/s)

STICKPOS: Control inceptor position.

1. Lateral Stick Position (%), +ve stick right.
2. Longitudinal Stick Position (%), +ve stick aft.
3. Collective Position (%), +ve up.
4. Pedal Position (%), +ve right pedal push.

Expected collective values were 0 - 100%. All other values are expected in the range +/-100%.

ACCELEROMETER: Simulator platform motion measurements. The sensor was located at the rear of the pod with the following orientation:

- a. Positive X = +ve forwards
- b. Positive Y = +ve left
- c. Positive Z = +ve up

Positive angles follow rule whereby if an observer looks along the positive linear axis, positive rotation is a clockwise motion.

1. Time tick value (nd)
2. Roll angle (deg)
3. Pitch angle (deg)
4. Yaw angle (deg)
5. X acceleration (g)
6. Y acceleration (g)
7. Z acceleration (g)
8. X angular rate (deg/s)
9. Y angular rate (deg/s)
10. Z angular rate (deg/s)

As such, there were 60 individual data values recorded per run.

Acknowledgements

The research reported in this paper is funded by the UK Engineering and Physical Sciences Research Council grant EP/D003512/1 (Rotorcraft-Pilot Couplings). The study is part of the University of Liverpool's contribution to GARTEUR H-AG16, Rotorcraft Pilot Couplings. The partner organisations would also like to acknowledge the test pilots (Mr. A. Berryman, Mr. S. Cheyne) who took part in

this study for their invaluable insights and continued hard work.

References

1. McFarland, M.W., *The Papers of Wilbur and Orville Wright*. 1st ed. 1953, New York: McGraw-Hill.
2. Lawrence, B. and G.D. Padfield. *Flight Testing Simulations of the Wright 1902 Glider and 1903 Flyer*. in *Annual Conference of the Society of Flight Test Engineers*. 2003. Annapolis, Maryland.
3. Lawrence, B. and G.D. Padfield, *Handling-Qualities Analysis of the Wright Brothers' 1902 Glider*. *Journal of Aircraft*, 2005. **42**(1): p. 224-236.
4. *Aviation Safety and Pilot Control: Understanding and Preventing Unfavorable Pilot-Vehicle Interactions*. National Research Council. 1997, Washington D.C.: National Academy Press.
5. Hamel, P. *Rotorcraft-Pilot Coupling, a critical issue for highly augmented helicopters? AGARD CP-592*. in *Symposium on Advances in Rotorcraft Technology*. 1996. Ottawa.
6. Dieterich, O., et al., *Adverse Rotorcraft-Pilot Coupling: Recent Research Activities in Europe*, in *34th European Rotorcraft Forum*. 2008: Liverpool, UK.
7. Pavel, M.D., et al., *Adverse Rotorcraft-Pilot Couplings - Prediction and Suppression of Rigid Body RPC*. *Sketches from the work of GARTEUR HC(AG16)*, in *34th European Rotorcraft Forum*. 2008: Liverpool, UK.
8. Serafini, J., et al., *Aeroelastic and Biodynamic Modelling for Stability Analysis of Rotorcraft-Pilot Coupling Phenomena*, in *34th European Rotorcraft Forum*. 2008: Liverpool, UK.
9. Mattaboni, M., et al., *Biomechanical pilot properties identification by inverse kinematics/inverse dynamics multibody analysis*, in *26th International Congress of the*

- Aeronautical Sciences*. 2008:
Anchorage, Alaska, USA.
10. Padfield, G.D. and M.D. White,
Flight simulation in academia; HELIFLIGHT in its first year of operation. The Aeronautical Journal of the Royal Aeronautical Society, September 2003. **107**(1075): p. 529-538.
 11. White, M.D. and G.D. Padfield,
Flight Simulation in Academia. Progress with HELIFLIGHT at the University of Liverpool, in *Flight Simulation 1929-2029: A Centennial Perspective*. 2004: RAeS, London, UK.
 12. Anon, *FLIGHTLAB Theory Manual (Vol. One)*. March 2004, Advanced Rotorcraft Technology: Mountain View, California.
 13. Padfield, G.D., et al., *Validation Criteria for Helicopter Real-time Simulation Models: Sketches from the work of GARTEUR HC-AG12*, in *30th European Rotorcraft Forum*. 2004: Marseilles, France.
 14. Anon., *Aeronautical Design Standard Performance Specification. Handling Qualities Requirements for Military Rotorcraft*. 21 March 2000, United States Army Aviation and Missile Command, Aviation Engineering Directorate.
 15. Mehl, H.J., et al., *PIO Experimental Evaluation of a Highly Augmented Aircraft*. December 2001, GARTEUR FM(AG-12) Technical Report TP-120-08.
 16. Hess, R.A., *Unified theory for aircraft handling qualities and adverse pilot coupling*. *Journal of Guidance, Dynamics and Control*, 1997. **20**(6).
 17. Mayo, J.R. *The involuntary participation of a human pilot in a helicopter collective control loop*. in *15th European Rotorcraft Forum*. 1989. Amsterdam, The Netherlands.
 18. Anon., *Guide to the Motionbase motion cueing algorithms*. 2000, Motionbase (Holdings) Ltd.